Electronic Supplementary Material (ESI) for New Journal of Chemistry.

Trigonelline hydrochloride conjugated onto PEGylated nanodiamond for a selective encapsulation efficiency and controlled release for inhibition of collagen fibrillation

*K. Rasheeda[a], Chandrasekar Inbasekar[a], Nishter Nishad Fathima[a]**

[a] Inorganic and Physical Chemistry Laboratory, Central Leather Research Institute, Council of Scientific and Industrial Research, Chennai, India

Corresponding Author

Tel.: +91 44 24437188; fax: +91 44 24911589.

E-mail addresses: nishad@clri.res.in, nishad.naveed@gmail.com (N.N. Fathima)

Experimental section

UV-Vis spectroscopy measurements

UV-1800 Shimadzu (UV-Visible spectrophotometer) of 1 cm path length was used to measure the aromatic group's absorption intensity in collagen between 200 to 400nm range. Native collagen and collagen-CND composites were incubated overnight at 4ºC followed by data recording and plotting using Origin 9 plus software.

Circular Dichroism Spectropolarimeter

The ability to understand potential differences introduced in the secondary and tertiary structure of collagen on the addition of CND was possible using a JASCO 815 Circular Dichroism Spectropolarimeter. About 400µl of the sample was inserted into quartz cuvette of 1mm path length and scanned for 0.2 nm per min speed along with three average scans per sample. Baseline correction was performed using acetate buffer followed by sample measurements from 190-260nm. The spectrum was recorded using spectra manager software and a graph of wavelength (nm) vs. molar ellipticity ($deg.cm^2.dmol^{-1}$) was plotted.

FT-IR (ATR) spectra analysis

FT-IR (ATR) is vibrational spectroscopy, which allows an understanding of the strength between covalent bonds and intermolecular forces in proteins. Native collagen and its composite at pH=4.5 were measured for its frequency and wavenumber shifts using JASCO FT/IR 4700 spectrometer. Around 60 scans on an average were performed with a time resolution of 4 cm^{-1} within 4000-500 cm^{-1}, a range of transmission mode.

Results and discussion

UV-Vis spectroscopy measurements

Collagen is a fibrous protein containing few aromatic residues such as tyrosine and phenylalanine so that it gives a weak absorption peak at 278nm [1]. The near UV absorption does not only measure its tyrosine content but also enunciates the integrity of non-helical telopeptide [2]. Figure S1 (a) illustrates the absorption spectra for native collagen and collagen-CND composites. This experiment was carried out at pH=4.5 since, at physiological pH, the self-assembled collagen fibrils would lead to an intense Tyndall scattering, thereby hindering recording of the UV spectrum of collagen.

A typical peptide absorption band approaches keto, amide and carboxylic acid residues involved in the polypeptide chains a characteristic native collagen peak at 219 nm [3]. A bathochromic shift of 224 nm was observed for collagen-CND5 (0.5%) predicting interaction between the carboxylic acid ends of CND with the positive polypeptide residues of collagen. Similarly, a typical peak of tyrosine at 278nm was seen to be masked by the carboxylic groups of CNDs upon its increasing concentration, as seen in figure S1 (b).

It is speculated that a shift or masking of the tyrosine peak may be due to the ionization of tyrosine to tyrosinate, which allows it to interact with the CNDs. Another reason for such a shift may be due to an increase in the solvation environment of collagen or a locally entrapped tyrosine molecule in a particular conformation involved in proton transfer [4]. On the other side, the absorbance of CNDs, with its increasing concentration illustrates a considerable hyperchromic shift, which increases the molar extinction coefficient compared to the native collagen. However, due to strong hydrogen-bonding interaction between the hydroxyl groups and aromatic rings of peptides [5].

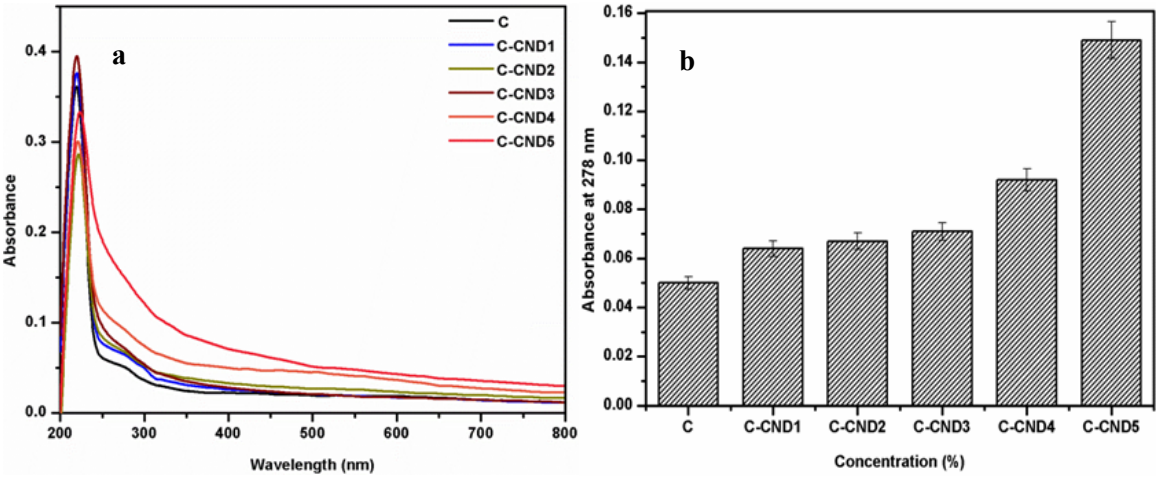

Figure S1. (a) Electronic spectra of collagen and its carboxylated nanodiamond composites with increasing concentrations (C-CND1 (1:0.02%) to C-CND5 (1:0.5%)) (b) Changes in the absorbance at 278 nm on addition on carboxylated nanodiamond

Secondary structural changes of collagen-carboxylated nanodiamond composites

The dichroic spectrum of the collagen-CND composite is given below in figure S2, with the inset showing molar ellipticity variation. As there is an increase in the concentration, the dichroic curves' intensity also shows a significant change with a linear decrease in molar ellipticity and an increase in Rpn values, as given in S3. Such a variation may be due to the plausible interaction between collagen and CND, which may be hydrogen or electrostatic in nature [6]. CND has an anionic surface charge capable of interacting with the positive residues of collagen. During the interaction, a slight disturbance was speculated in the microenvironment of collagen, with a decrease in molar ellipticity and Rpn ratio increase. This would ensure the interaction of CND functional groups near the basic residues of collagen. Therefore, in the case of ND, conformational stability is confirmed only up to C-CND2 (1:0.05%), in which the affinity of CND towards collagen end residues become high enough to cause aggregation and solvation effects around it.

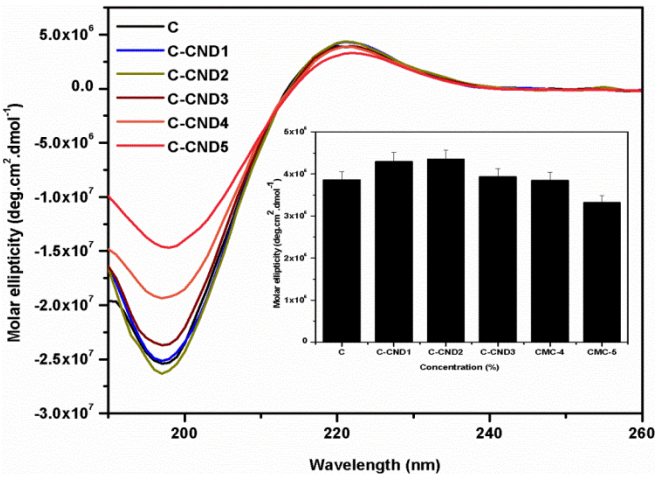

Figure S2. Changes in the far-UV CD of native collagen (C) and collagen carboxylated nanodiamond composites (C-CND1 (1:0.02%) to C-CND5 (1:0.5%)) as a function of wavelength with an inset comprising of the plot of molar ellipticity at 222nm vs varied concentrations of composites (C-CND1 (1:0.02%) to C-TQ5 (1:0.5%))

Sample code	% Concentration	Rpn values
C	(1:0)	0.15
C-CND1	(1:0.02)	0.17
C-CND2	(1:0.05)	0.17
C-CND3	(1:0.1)	0.17
C-CND4	(1:0.3)	0.20
C-CND5	(1:0.5)	0.22

Table S3. Rpn values of collagen with different molar ratios of carboxylated nanodiamond

FT-IR (ATR) measurements

A broad absorbance over different vibrational levels of nanodiamonds (NDs) takes place from its core and its active surface. In terms of CND, the active surface species are carboxyl groups showing a cluster peak around 1600 $cm^{-1}$and a broad peak at 3301 cm^{-1}, which shows hydroxyl

groups undergoing OH stretching and bending. Similarly, a minor peak around 2900 cm^{-1} was noticed depicting a CH, CH_2, and CH_3 symmetric and asymmetric stretching [7-8], as illustrated in figure S4(b). There are four major absorption modes of collagen, as in, characteristic amide A peak at 3279 cm^{-1}confirms the N-H vibrational stretching corresponding to those hydrogen systems engaged in core stability of collagen polypeptide backbone. The peak at 1636 cm^{-1} is an amide I band showing the hallmark of collagen structural compactness. It depicts a C=O stretching vibration and N-H bending coupled with deformations of individual functional group residues present along the carbonyl backbone of collagen. Amide II bands at 1564 cm^{-1}were observed to confirm the presence of inter-and intra-molecular hydrogen bonds indicating N-H bending coupled with C-N stretch. The final mode of vibration falls under a complex fingerprint region of collagen at 1240 cm^{-1}, known as amide III. A couple of intense N-H stretching, bending and deformation vibrations are noticed coupled with C-N bending and C-O stretching [9].

As shown in the figure below S4 (a), precise shifts have been seen in the vibrational levels. A peak shift in amide A from C-CND1 to C-CND5 is about 3 cm^{-1}, which is not a significant shift whereas amide I show 3 cm^{-1}shift, amide II shows 2 $cm^{-1}$and amide III illustrates a 2 cm^{-1}shift. However, an 8 cm^{-1} shift was noted to increase from control to C-CND1, ensuring an acute interaction of ND's carboxyl ends with the N-H end residues of collagen.

Speculating the mechanism of interaction between CND and collagen is a fascinating fact since the hydration network of both is highly organized. It is reported that CND is quiet affirmative towards the electrostatic bonding with the hydrogen of water molecules forming a tetrahedral bond much similar to the ice-like formation. Collagen type I is a well-known protein for its intense hydration network shielding the alpha-helix structure integrity from the extreme conditions to avoid denaturation. In such a case, two possibilities may be predicted; one is an electrostatic

interaction of C=O bond as it will be negatively charged at the acidic pH and will have actual negative charges to interact with the hydrogen belonging to the water molecule of collagen. A second possibility is an interaction between C=O of CND and N-H polar residues of the terminal polypeptide chains and the ones exposed to the surface of the collagen such as arginine, histidine, and lysine. Therefore, CND demonstrates its affinity towards collagen to be significant enough to maintain its solvation environment and stabilize it via hydrogen and electrostatic interaction.

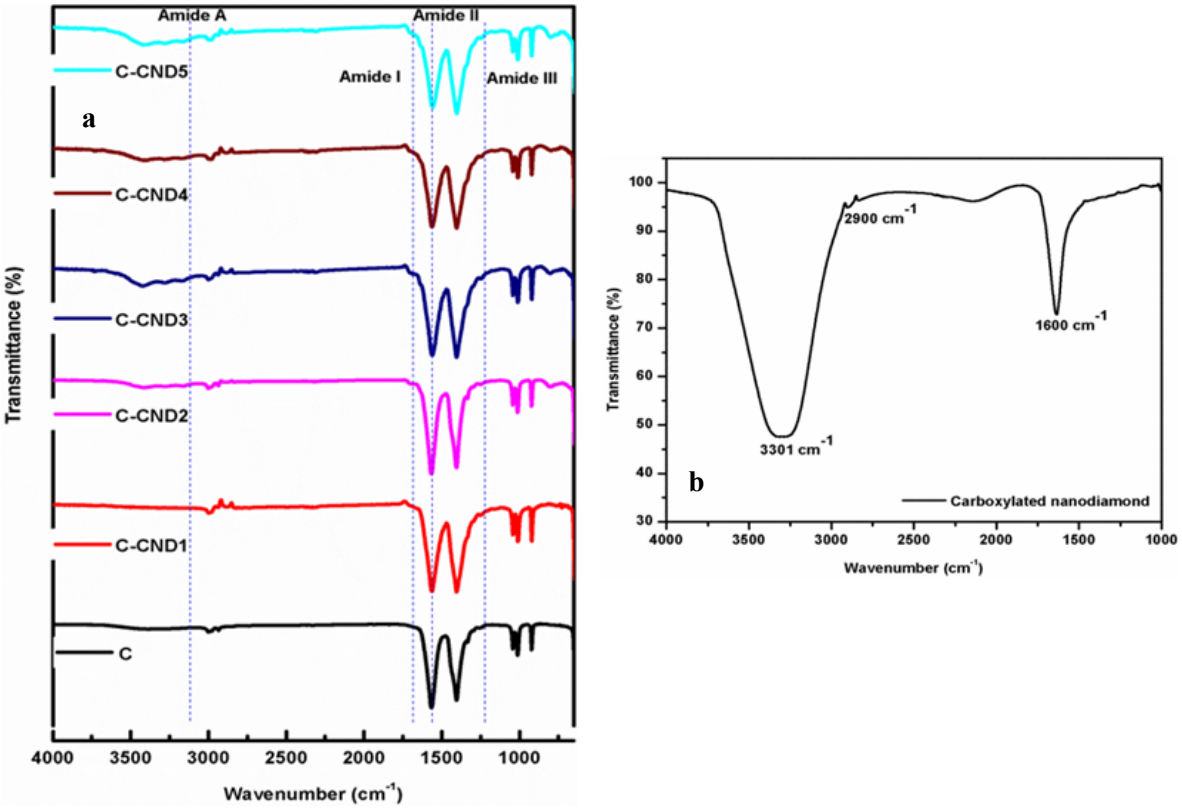

Figure S4. FT-IR (ATR) spectrum (a) of native collagen solution (C) at pH=4.5 along with the addition of carboxylated nanodiamond (C-CND1 (1:0.02%) to C-CND5 (1:0.5%)) (b) FT-IR (ATR) spectrum of pure carboxylated nanodiamond

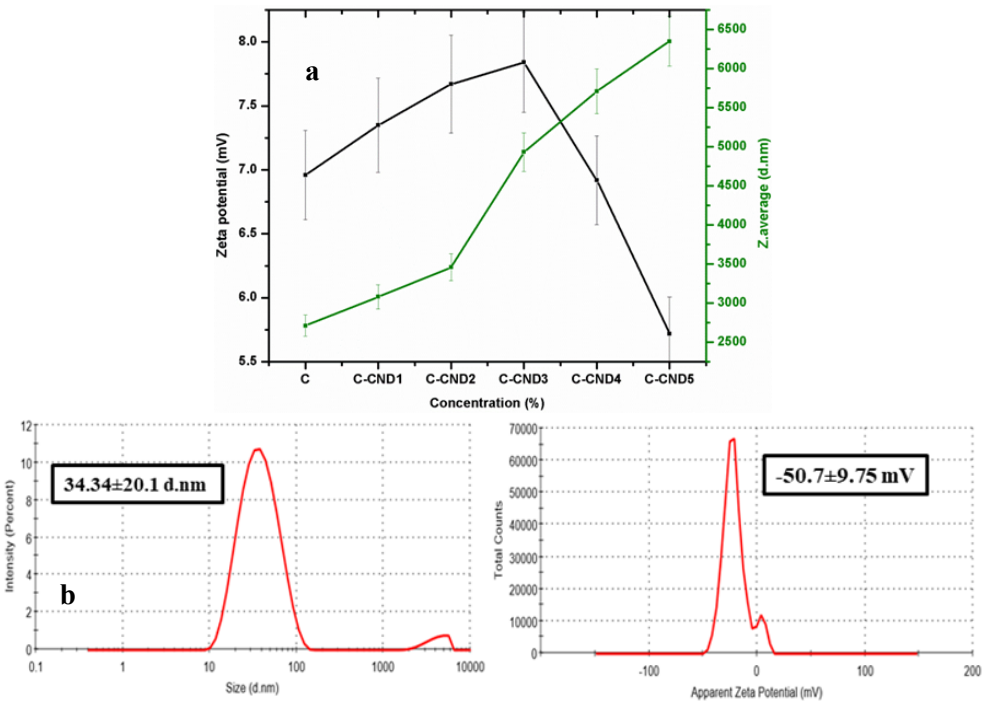

Figure S5. Hydrodynamic diameter and zeta potential (a) of native collagen solution (C) at pH=4.5 along with the addition of carboxylated nanodiamond (C-CND1 (1:0.02%) to C-CND5 (1:0.5%)) (b) of pure carboxylated nanodiamonds (CND)

Table S6. Summary of concentration of TGH, encapsulation efficiency of nanodiamond and amount of TGH loaded on to CND-PEGDA

Sample (CND-PEGDA-TGH hybrid)	Concentration (μg)	Encapsulation efficiency (wt. %)	Amount of drug loaded (μg)
CPT-1	5	96.8±0.4	0.00682±0.1
CPT-2	10	98.4±0.3	0.00984±0.1
CPT-3	15	98.9±0.2	0.01484±0.2
CPT-4	20	99.2±0.3	0.01984±0.4
CPT-5	25	99.3±0.2	0.02488±0.4
CPT-6	30	99.4±0.2	0.03315±0.5
CPT-7	35	99.5±0.1	0.03483±0.5
CPT-8	40	99.6±0.1	0.03984±0.5

Table S7. DLS parameters hydrodynamic diameter and zeta potential of collagen-carboxylated nanodiamond composites

Sample	DLS parameters	
	Hydrodynamic diameter (d. nm)	Zeta potential (ζ) (mV)
CND	34.34±20.1	-50.7±9.75
C	2712±7.8	6.96±4.91
C-CND1 (1:0.02%)	3081±6.02	7.35±6.54
C-CND2 (1:0.05%)	3459±5.52	7.67±5.16
C-CND3 (1:0.1%)	4932±10.09	7.84±5.65
C-CND4 (1:0.3%)	5709±7.62	6.92±5.80
C-CND5 (1:0.5%)	6349±36.24	5.72±5.52

At pH 4

Results

		Mean (mV)	Area (%)	St Dev (mV)
Zeta Potential (mV): -3.51	Peak 1:	-3.51	100.0	14.7
Zeta Deviation (mV): 14.7	Peak 2:	0.00	0.0	0.00
Conductivity (mS/cm): 1.37	Peak 3:	0.00	0.0	0.00

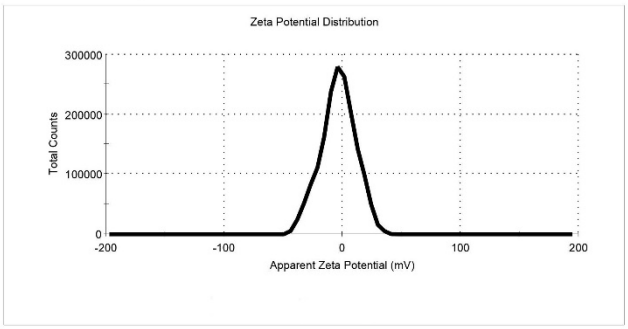

At pH 7

Results

		Mean (mV)	Area (%)	St Dev (mV)
Zeta Potential (mV): -31.4	Peak 1:	-31.4	100.0	15.2
Zeta Deviation (mV): 15.2	Peak 2:	0.00	0.0	0.00
Conductivity (mS/cm): 1.88	Peak 3:	0.00	0.0	0.00

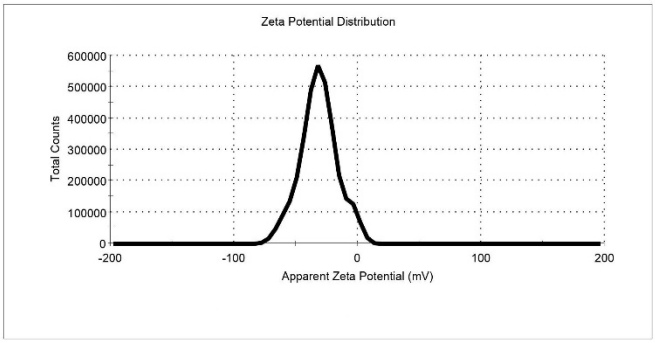

At pH 12

Results

		Mean (mV)	Area (%)	St Dev (mV)
Zeta Potential (mV): -56.7	Peak 1:	-56.7	100.0	19.2
Zeta Deviation (mV): 19.2	Peak 2:	0.00	0.0	0.00
Conductivity (mS/cm): 0.279	Peak 3:	0.00	0.0	0.00

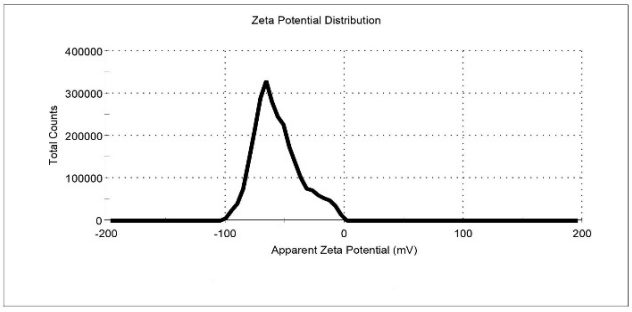

Figure S7 Zeta potential of drug conjugated CND at different pH

REFERENCES

[1] S. Lindy, T. Sorsa, K. Suomalainen, A. Lauhio and H. Turto, Eur. J. Inorg. Chem. 156 (1986) 1-4.

[2] G.C. Na, Top. Catal. 8 (1988) 315–330.

[3] A. Veeruraj, M. Arumugam and T. Balasubramanian, Process Biochem. 48 (2013) 1592–1602.

[4] C.M.P. Vidal, W. Zhu, S. Manohar, B. Aydin, T.A. Keiderling, P.B. Messersmith and A. K Bedran-Russo, Acta Biomater. 41 (2016) 110–118.

[5] M.E. Plonska-Brzezinska, D.M. Bobrowska, A. Sharma, P. Rodziewicz, M. Tomczyk, J. Czyrko and K. Brzezinski, RSC Adv. 5 (2015) 95443–95453.

[6] T. Petit, L. Puskar, T. Dolenko, S. Choudhury, E. Ritter, S. Burikov and E.F. Aziz, J. Chem. Phys. 121 (2017) 5185–5194.

[7] O. Kuznetsov, Y. Sun, R. Thaner, A. Bratt, V. Shenoy, M.S. Wong and W.E. Billups, Langmuir, 28 (2012) 5243–5248.

[8] Z. Rastian, S. Pütz, Y.J. Wang, S. Kumar, F. Fleissner, T. Weidner and S.H. Parekh, ACS Biomater. Sci. Eng. 4 (2018) 2115–2125.

[9] K.A. Laptinskiy, E.N. Vervald, A.N. Bokarev, S.A. Burikov, M.D. Torelli, O.A. Shenderova and T. A. Dolenko, J. Phys. Chem. C. 122 (2018) 11066–11075.